Drought variability in the Pacific Northwest from a 6,000-yr lake sediment record

Daniel B. Nelson[a,1], Mark B. Abbott[a,2], Byron Steinman[a], Pratigya J. Polissar[b], Nathan D. Stansell[a,c], Joseph D. Ortiz[d], Michael F. Rosenmeier[a], Bruce P. Finney[e], and Jon Riedel[f]

[a]Geology and Planetary Science, University of Pittsburgh, 4107 O'Hara Street, Room 200, Space Research Coordination Center, Pittsburgh, PA 15260; [b]Lamont–Doherty Earth Observatory, Columbia University, 61 Route 9W, Palisades, NY 10964; [c]Byrd Polar Research Center, Ohio State University, 1090 Carmack Road, Columbus, OH 43210; [d]Department of Geology, Room 334/336 McGilvrey Hall, Kent State University, Kent, OH 44242; [e]Biological Sciences and Geosciences, Idaho State University, Pocatello, ID 83209; and [f]United States Park Service, North Cascades National Park, Marblemount, WA 98267

Edited by James P. Kennett, University of California, Santa Barbara, CA 93106, and approved January 18, 2011 (received for review June 28, 2010)

We present a 6,000-yr record of changing water balance in the Pacific Northwest inferred from measurements of carbonate $\delta^{18}O$ and grayscale on a sediment core collected from Castor Lake, Washington. This subdecadally resolved drought record tracks the 1,500-yr tree-ring-based Palmer Drought Severity Index reconstructions of Cook et al. [Cook ER, Woodhouse CA, Eakin CM, Meko DM, Stahle DW (2004) *Science* 306:1015–1018] in the Pacific Northwest and extends our knowledge back to 6,000 yr B.P. The results demonstrate that low-frequency drought/pluvial cycles, with occasional long-duration, multidecadal events, are a persistent feature of regional climate. Furthermore, the average duration of multidecadal wet/dry cycles has increased since the middle Holocene, which has acted to increase the amplitude and impact of these events. This is especially apparent during the last 1,000 yr. We suggest these transitions were driven by changes in the tropical and extratropical Pacific and are related to apparent intensification of the El Niño Southern Oscillation over this interval and its related effects on the Pacific Decadal Oscillation. The Castor Lake record also corroborates the notion that the 20th century, prior to recent aridity, was a relatively wet period compared to the last 6,000 yr. Our findings suggest that the hydroclimate response in the Pacific Northwest to future warming will be intimately tied to the impact of warming on the El Niño Southern Oscillation.

lake sediment | oxygen isotope

Recent droughts that affected the American west were among the most severe on record (1–3). This aridity, combined with rapid population growth and limited water resources, provides the impetus to improve our understanding of long-term moisture balance to better predict and plan for future droughts and wet periods. Evidence suggests that drought in North America is strongly influenced by synoptic-scale changes in atmosphere-ocean dynamics (4), with El Niño events associated with drier conditions in the northwest and La Niña conditions being conducive to drought in much of the arid southwest (2). Documenting decadal-scale aridity patterns over several millennia will improve knowledge of drought frequency, duration, and magnitude, and improve our understanding of how these characteristics respond to long-term changes in the influential Pacific climate patterns, such as the El Niño Southern Oscillation (ENSO) and the Pacific Decadal Oscillation (PDO).

Model projections of global precipitation patterns in the coming century predict an intensification of zonal midlatitude precipitation bands as well an intensification of subtropical aridity, and an accompanying poleward shift of these patterns in response to increased greenhouse gas concentrations (5). Additional constraints on the degree to which drought cycles are controlled by extraregional teleconnections as opposed to zonal mean conditions will help to improve the predictive capability of climate models to differentiate between these interacting controls.

Most knowledge of preinstrumental-period drought comes from moisture-sensitive, annually dated tree-ring records that allow precise regional comparison and data synthesis (1, 6–8). Tree-ring based reconstructions of the Palmer Drought Severity Index (PDSI), a widely used tool for assessing water balance (1), are available in a gridded network over North America for the past approximately 500 to 2,000 yr (9). Despite the outstanding quality of these data, tree-ring studies are constrained by the life span of trees and uncertainty generally increases with age due to limited numbers of old samples. Lake sediments are not subject to the same shortcomings, and also provide an independent source of precipitation-sensitive proxy data with which to evaluate past climate. Moreover, such records span the Holocene and are sensitive recorders of the regional balance between precipitation and evaporation (P/E).

Castor Lake Physical Setting

Castor Lake (48.54° N, 119.56° W; elev. 594 m) is a small (approximately 0.07 km^2) closed-basin (low outseepage rate and no surficial outflow) oligosaline (>2,000 mg/L) system located just east of the Cascade Range in the Pacific Northwest (PNW). The catchment (0.86 km^2) occupies a plateau several hundred meters above the surrounding region, isolating it from distal sources of groundwater and restricting hydrologic input to precipitation, runoff, and catchment groundwater. Lake water δD and $\delta^{18}O$ data, as well as hydrologic modeling of Castor Lake, indicates that evaporation is the major water-loss pathway (10). Spatial correlations generated from the results of a tree-ring-based reconstruction of the PDSI (9) show that Castor Lake is situated within a region that should be representative of the greater PNW but is anticorrelated with patterns of aridity in the desert Southwest. The geochemical and hydrologic condition of the lake causes annual water-column carbonate precipitation. X-ray diffraction and scanning electron microscopy identified aragonite as the only sedimentary carbonate mineral present in abundant quantities.

In Castor Lake the $\delta^{18}O$ of aragonite primarily reflects lake water $\delta^{18}O$ and hence the P/E influencing the system at the time

Author contributions: M.B.A., B.P.F., and J.R. designed research; D.B.N. and N.D.S. performed research; B.S., P.J.P., and M.F.R. contributed new reagents/analytic tools; D.B.N., B.S., P.J.P., and J.D.O. analyzed data; and D.B.N., M.B.A., J.D.O., M.F.R., and B.P.F. wrote the paper.

The authors declare no conflict of interest.

This article is a PNAS Direct Submission.

Data deposition: The age control, isotope, and grayscale data reported in this paper have been deposited in the NOAA World Data Center for Paleoclimatology electronic data archive, ftp://ftp.ncdc.noaa.gov/pub/data/paleo/paleolimnology/northamerica/usa/washington/castor2011.txt.

[1]Present address: School of Oceanography, University of Washington, Box 355351, Seattle, WA 98195.

[2]To whom correspondence should be addressed. E-mail: mabbott1@pitt.edu.

This article contains supporting information online at www.pnas.org/lookup/suppl/doi:10.1073/pnas.1009194108/-/DCSupplemental.

of mineral formation. Most aragonite precipitates at similar temperatures during summer months, minimizing the influence of water temperature variations. Monitoring of the lake water $\delta^{18}O$ since 2003 revealed large isotopic shifts concordant with regional hydroclimate. Hypolimnetic anoxia inhibits sediment bioturbation so the $\delta^{18}O_{aragonite}$ signal integrates water isotopic composition over the lake residence time, which we estimate to be approximately 3 yr based on our isotopic mass balance modeling studies of the lake (10, 11) and comparison with analogous systems (12). We corroborated the regional nature of changes in the sediment record from Castor Lake $\delta^{18}O_{aragonite}$ by comparison with $\delta^{18}O$ values in ostracods in a sediment core from Scanlon Lake, situated in an adjoining watershed, and confirmed our interpretation of the influence of regional hydroclimate on these systems through comparison with nearby instrumental precipitation and PDSI data (Fig. 1). The PDSI was developed as a method of calculating theoretical soil moisture, and as such is a calculation of water balance that incorporates the cumulative effects of precipitation, temperature, soil moisture, and evapotranspiration (13). As the $\delta^{18}O$ of Castor Lake is also a function of water balance, it is logical that the two measures should largely covary. The PDSI is also correlated with carbonate precipitation rates in basins with characteristics similar to Castor Lake (14). Finally, the PDO instrumental data generally tracks lacustrine $\delta^{18}O$ from both lakes as well as the precipitation and PDSI data, supporting the assertion that the PDO shifts during the 20th century impacted the P/E balance of the region (15).

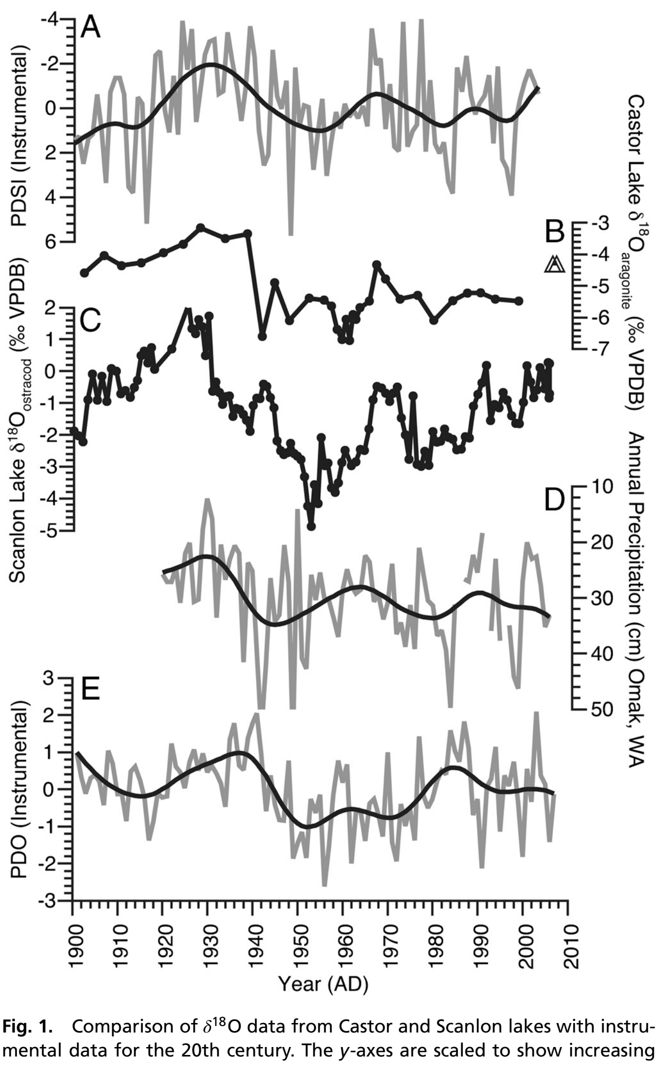

Fig. 1. Comparison of $\delta^{18}O$ data from Castor and Scanlon lakes with instrumental data for the 20th century. The *y*-axes are scaled to show increasing aridity to the top. (*A*) Instrumental record of the PDSI from central Washington with a 20-yr low-pass filter. (*B*) The last 100 yr of the 6,000-yr detrended Castor Lake carbonate $\delta^{18}O$ record measured on authigenic aragonite. Average 2005–2006 A.D. sediment trap $\delta^{18}O$ values shown as open triangles. (*C*) The last 100 yr of the $\delta^{18}O$ record from Scanlon Lake measured on ostracod carapaces. (*D*) Total annual precipitation from the Omak, Washington airport 9 km south of Castor Lake. (*E*) Instrumental record of the PDO index with 20-yr low-pass filter (22).

Higher/lower sediment image grayscale values, indicative of correspondingly darker/lighter sediment, tend to occur when $\delta^{18}O$ values are also high/low (Fig. 2 and Figs. S1 and S2). Interpretations of inorganic carbonate precipitation in lakes often suggest increased carbonate formation under evaporation-driven lake-level decreases caused by concentration of dissolved ions. However, carbonate precipitation can be controlled by groundwater-mediated Ca^{2+} supply in small alkaline lakes, which may lead to Ca^{2+} limitation during dry phases (14). Castor Lake sediment trap (Fig. 2) and instrumental data (Fig. 1) are consistent with this model, indicating that dark layers are formed during arid periods when reduced Ca^{2+} input from groundwater leads to a decline in aragonite precipitation (14) (Fig. S1). The changes in the grayscale record support our interpretation that the dominant control on lake water $\delta^{18}O$ is P/E and not temperature or the source of precipitation, as these latter factors should not produce a change in sediment composition. Detailed hydrologic and isotopic modeling of Castor Lake confirm that precipitation is the primary control on lake water $\delta^{18}O$ due to two factors: the high isotopic sensitivity of the lake catchment system to hydrologic changes, which are primarily controlled by precipitation, and the much larger variance in interannual precipitation relative to temperature and humidity (10). Because carbonate deposition is controlled primarily by Ca^{2+} supply, which increases when groundwater inflow increases under wetter climate conditions, rain, and snowfall are the primary controls on the grayscale record. In contrast, the $\delta^{18}O_{aragonite}$ is controlled by precipitation as well as relative humidity and temperature changes that affect evaporation rates, but the latter two climate variables have a relatively small effect in this system (10). Although their controls are similar, the slight differences explain the minor discrepancies between the grayscale and $\delta^{18}O_{aragonite}$ measurements. Based on our modern-system calibrations (Fig. 1), hydrologic and isotopic modeling efforts of Castor Lake (10, 11), and our understanding of the processes controlling sediment deposition, we suggest that the Castor Lake grayscale record may be interpreted as a proxy of regional hydroclimate.

Results and Discussion

Higher $\delta^{18}O$ values at Castor Lake, indicating drier conditions, correspond to lower PDSI values, also indicative of reduced moisture availability. Covariance between sediment $\delta^{18}O$ and grayscale is consistent with our model of climatic controls on lake sediment composition (Fig. 2 and Figs. S1 and S2) and thus suggests that the grayscale values should also negatively correlate with the PDSI. This relationship permits comparison of the high-

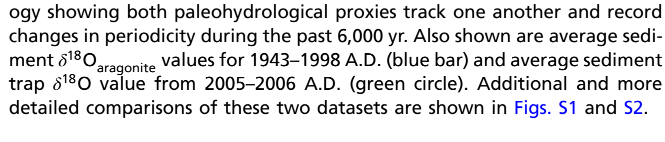

Fig. 2. Normalized Castor Lake carbonate $\delta^{18}O_{aragonite}$ (red line) and grayscale (black line) on the radiocarbon, ^{137}Cs, teprha, and PDSI-tuned chronology showing both paleohydrological proxies track one another and record changes in periodicity during the past 6,000 yr. Also shown are average sediment $\delta^{18}O_{aragonite}$ values for 1943–1998 A.D. (blue bar) and average sediment trap $\delta^{18}O$ value from 2005–2006 A.D. (green circle). Additional and more detailed comparisons of these two datasets are shown in Figs. S1 and S2.

er resolution grayscale signal from Castor Lake with the annually resolved network of PDSI reconstructions (1). The nearest grid point, #43, is located approximately 120 km to the south (Fig. 3*D*), and spans approximately 1,500 yr. Not surprisingly, chronological uncertainties inherent to radiocarbon dating result in relatively poor correlation [degrees of freedom (DOF) = 1318, $r = -0.10$, $p = 0.0002$] between the Castor Lake grayscale record and the PDSI reconstruction. However, minor adjustments in the lake sediment core chronology improve this correlation (DOF = 1318, $r = -0.70$, $p < 0.0001$) (*SI Materials and Methods* and Fig. S3). Age adjustment (i.e. tuning) is justified by the observed anticorrelation at sediment depths where accurate age control is provided by ^{137}Cs and tephra layers of known age. Adjustments in the chronology were within the 2σ error range of calibrated radiocarbon dates, and no dates were abandoned in favor of forced anticorrelation to the PDSI. The anticorrelation is maintained even after adjusting for artificial skill (DOF = 53, adjusted $r = -0.67$, $p < 0.0001$) (Fig. 3*A*). The comparison is included primarily to confirm that the two approaches to reconstructing paleoaridity document similar variability within the dating uncertainty of the lake record.

The similar patterns in PDSI and grayscale prior to the instrumental period strengthens the interpretation of grayscale values as an indicator of relative changes in water balance over the past 6,000 yr, and serves as independent method validation for both the tree-ring and lake-sediment data. The ability to attain significant anticorrelation over the 1,500-yr overlap also demonstrates that Castor Lake is responding to regional climate rather

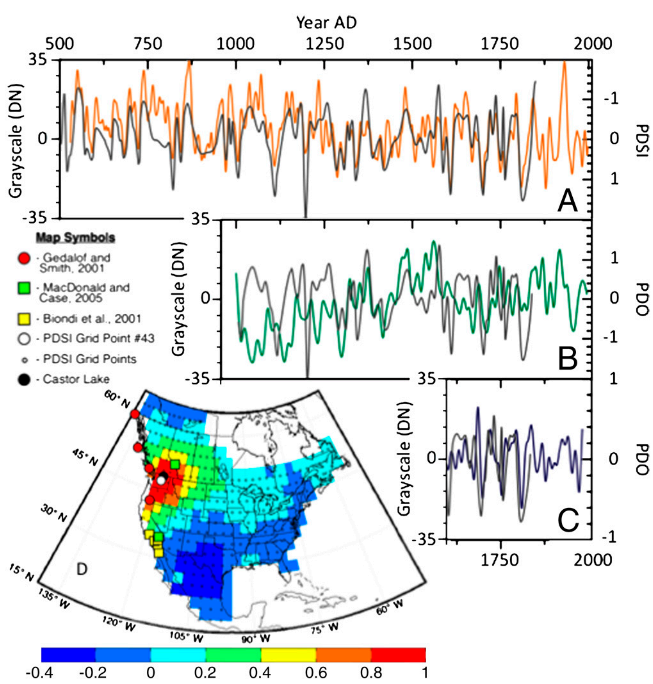

Fig. 3. Comparison of the tuned-chronology Castor Lake grayscale record with tree-ring reconstructions of the PDSI and PDO. Grayscale record (black line) compared to (*A*) PDSI grid point #43 reconstruction by Cook et al. (9) with y-axis reversed, such that increasing aridity is shown as upward trends (orange) (*B*) McDonald and Case (19) PDO reconstruction (green), (*C*) Gedalof and Smith (17) PDO reconstruction (blue). All data were 20-yr low-pass filtered to improve visualization (*SI Materials and Methods*). (*D*) The contrasting hydroclimate of the Pacific NW with the desert Southwest is illustrated by the map generated from the correlation of grid point #43 in the PNW with other grid points from the tree-ring-based reconstruction of the PDSI (9), which shows opposite patterns of aridity in the two regions based on data for the period between 1645–1900 A.D. Locations of field sites for North American PDO reconstructions are indicated (see map legend), as well as PDSI grid points, and the location of Castor Lake.

than local catchment dynamics. As a test of this regional significance, a correlation map between each PDSI site and grid point #43 was generated for the entire PDSI network (Fig. 3*D*). Results confirm strong coherent regional behavior in the PNW, and also illustrate the moderate negative correlation between the region and portions of the American west, particularly southern Texas and northern Mexico. This supports our assertion that the Castor Lake drought record can be used to document drought history for the greater PNW region, with drought being defined in this case as periods with positive grayscale values.

The well-dated, high-resolution Castor Lake grayscale record spanning the past 6,000 yr can be interpreted in the context of changes in regional, decadal-scale variability in effective moisture. To this end, we applied wavelet analysis to explore changes in event periodicity (16) (Fig. 4*A*). Although direct correlation of individually resolved drought events from the grayscale data to other proxy records is hindered by radiocarbon dating uncertainties, minor age offsets do not significantly affect assessments of changes in variability over centennial to millennial timescales. Wavelet analyses of the grayscale series, using different preprocessing assumptions and randomized age-models, illustrate the fact that the chronological uncertainty in our data does not influence the results (Fig. S4). Frequency ranges with elevated spectral power were identified from the global wavelet (Fig. 4*B*) and further analyzed for scale-averaged wavelet power. Results demonstrate that strong periodicities in the multidecadal (16–64-yr) band during the middle Holocene become gradually weaker around 4,000 cal yr B.P. (Fig. 4*C*). Moreover, the centennial (72–128-yr) band appears insignificant throughout much of the record (Fig. 4*D*). This centennial component, which partially characterizes North Pacific variability in most proxy reconstructions spanning the past 1,000 yr (17–19), exhibits greater average power in the last millennium than during any other period in the past 6,000 yr. Additionally, the intermittent nature of this centennial scale component, as observed in the wavelet analysis from Castor Lake, is consistent with other proxy records spanning the last 1,000 yr (19). This evolving pattern of drought cyclicity over the 6,000-yr record may partially reflect precessional insolation forcing, but may also be driven in part by changing synoptic climate patterns of unknown origin.

The transition to lower frequency and longer duration wet/dry cycles that occurred in the last millennium is coincident with increased drought magnitude between 900 and 1300 A.D. (1,050 and 650 B.P.), as suggested by tree-ring indicators of drought across the large area of the American west (1). This increased drought severity may have resulted from prolonged moisture balance excursions away from mean state values, which provide more time for cumulative effects to build (e.g., successive years with lower than average precipitation totals). Comparison of instrumental-period stable isotope data with the full sediment sequence highlights the middle and late 20th century wet phase as one of the more extreme events of the past 6,000-yr (Fig. 2). Overall, the 6,000-yr grayscale record shows that droughts on average are more likely to last longer than wet periods (Fig. S5). For example, over the last 6,000 yr, 25% of droughts, compared to 19% of wet periods, last longer than 30 yr.

Many of the drought events in the PNW and the American west are correlated with Pacific Ocean dynamics such as ENSO (2). For example, dry periods commonly occur when a high-pressure ridge forms over the northeastern Pacific and prevents moist air from entering the region (8). The Pacific westerlies, driven in part by the pressure gradient between the Aleutian low and the North Pacific high-pressure systems, exert a strong influence on PNW climate (20). Decadal fluctuations in precipitation account for 20–45% of annual precipitation variance in western North America (21), and the regional water balance strongly correlates with the PDO (4, 22). Thus decadal-scale changes in the Castor Lake P/E record are likely to be at least partially controlled by

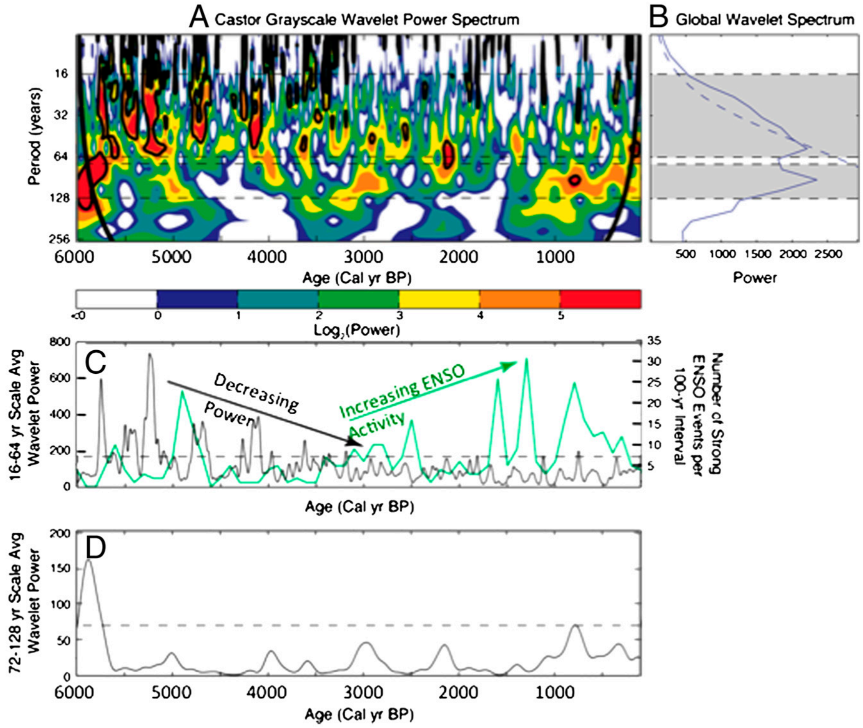

Fig. 4. (*A*) Wavelet analysis of the Castor Lake grayscale record. Data were detrended and normalized to the mean prior to wavelet analysis as described in the text, but not filtered. Areas outlined in black are significant at the 95% level, and the cone of influence is designated by thick black lines (16). Dashed horizontal lines define regions used in scale average plots shown in C and D, as determined through data-adaptive peak identification in the global wavelet spectrum in panel B. (*B*) Global wavelet spectrum with scale average bands defined by shaded area and dashed black lines. Dashed blue line represents 95% confidence interval for the global wavelet spectrum. (*C*) Multidecadal (16–64-yr) scale average wavelet power (black) shown with ENSO activity record from ref. 32. (*D*) Centennial (72–128-yr) scale average wavelet power.

decadal variability of the Pacific Ocean, expressed regionally by variability associated with ENSO and the related PDO. Comparison of sediment and climate data with the PDO index supports this conclusion (Fig. 1). Although the Atlantic Multidecadal Oscillation has been shown to act in concert with the PDO in influencing precipitation and drought over much of the western United States, the strength of this interaction in the PNW is weak and the PDO is the dominant driver, historically (4). Drought frequency in the PNW has also been shown to correlate with northern hemisphere temperature, where increasing temperature corresponds to decreasing drought recurrence during the instrumental period (4).

Because drought events in the PNW have been linked to warm phases of the PDO (4, 22), it follows that the Castor Lake grayscale record and tree-ring inferred PDSI values should correlate with regional PDO reconstructions, which are available from a number of widely distributed study sites (Fig. 3). However, coherence among the reconstructions is poor, a likely result given the underdeveloped state of understanding of the long-term influence of the PDO on regional climate and the potential for changes in the spatial impact on North American climate through time. Regardless, the records are useful indicators of hydroclimate, and of these the Castor Lake grayscale record shows the strongest correlation with the PDO reconstruction derived from tree chronologies in coastal Oregon, British Columbia, and Alaska (17) (Fig. 3). Weaker correlations exist with reconstructions that rely on tree chronologies from the southwestern United States (19, 23) and Asia (24, 25) (Fig. 3). These relationships are consistent with the regional PDSI correlation pattern and support the inference that each PDO reconstruction preserves local expressions of multidecadal variability (24). The strongest correlation with the proximal reconstruction of Gedalof and Smith (17) confirms that Castor Lake P/E is influenced by changes in multidecadal climate variability as expressed in the PNW.

The influence of extratropical and tropical Pacific climate on drought conditions in the PNW (2, 26, 27) suggests that changes in multidecadal drought periodicity observed at Castor Lake are related to Pacific Ocean variability over the past 6,000 yr. A relationship between ENSO and the PDO is suggested by the positive correlation between El Niño events and warm PDO phases over the past 400 yr (28). Further, the PDO has been modeled as the decadal-scale response in the midlatitudes to ENSO forcing combined with atmospheric noise (29). If the PDO does represent the midlatitude ocean response to ENSO, it would follow that changes in the ENSO system would lead to changes in the PDO (even if the PDO itself is not a true dynamical mode of climate variability) and that such changes would be recorded in the Castor Lake grayscale record. A variety of Pacific proxy records suggest muted middle Holocene ENSO variability. These include oxygen isotope measurements on individual planktonic foraminifera from sediments collected in the eastern tropical Pacific (30), oxygen isotope measurements on fossil corals in the western equatorial Pacific (31), as well as the sedimentology of Laguna Palcacocha, Ecuador, which suggests a gradual increase in the number of strong ENSO events over the Holocene (32). These changes are coincident with the gradual decline observed in the strength of the multidecadal component of drought variability at Castor Lake (Fig. 4*C*), and suggest significant basin-scale changes in the Pacific Ocean between approximately 4,000 and 3,000 cal yr B.P., and to a lesser extent, at approximately 1,000 cal yr B.P. These ideas are consistent with a recent synthesis study of proxy data and model results associated with middle Holocene ENSO intensification from 4,500 to 3,500 cal yr B.P., which suggest an increase in insolation-driven Indo-Pacific warming as a possible mechanism (33). The results from Castor Lake highlight the fact that the semicyclic moisture balance of the last millennium may not persist through changing ENSO mean states, or the projected poleward shift of the midlatitude precipitation pattern in the coming century (5).

Conclusions

Today ENSO has a clear impact on western North American climate and is the dominant control on interannual climate variability worldwide. Improved understanding of the long-term behavior of this system and how it responds to external forcing are among the most important issues in reducing uncertainty in climate change projections. The data from Castor Lake document changing drought cycles in the PNW over the last 6,000 yr that were likely driven by the evolution of ENSO and its teleconnections with the PNW, thus confirming the long-term sensitivity of the region to activity in the tropical Pacific. The scale and pace of these changes suggest a large and gradual forcing mechanism such as precessional insolation. Altering the evolution of wet/dry cycles that has operated for the past 6,000 yr would therefore seem to require a global-scale mechanism. Anthropogenic changes in radiative forcing may be of such a scale, although the specific nature of ENSO response to such changes cannot yet be predicted with confidence (34). However, our data confirm that teleconnections with the PNW are a robust feature of the ENSO system, and therefore that any change in ENSO is likely to have a profound impact on water availability, people and economies in the circum-Pacific region.

Materials and Methods

Two sediment cores were collected from Castor Lake in 2003 using a Livingston corer. Unconsolidated surface sediments were recovered in 2004 with a freeze corer. Sediment chronology was established by 11 calibrated (35) accelerator mass spectrometer ^{14}C dates on terrestrial macrofossils, tephrochronology and ^{137}Cs (*SI Materials and Methods*, Table S1, and Fig. S6). The upper 2.5 m of sediment, spanning the last approximately 6,000 yr, is comprised of millimeter to sub-millimeter-scale laminations indicating that the sediment record is preserved at nearly annual resolution. Prior to approximately 6,000 cal yr B.P. laminations transition to irregular, mottled and banded deposits, indicating bioturbation and mixing caused by a lower lake level prior to this time. Loss on ignition analyses, a rough estimate of organic matter and carbonate content, were conducted at 1–2 cm resolution throughout the record. Carbonate content averaged 60–70% by weight, and organic matter averaged 20–30%. Smear-slide analyses identified biogenic silica (i.e., diatom frustules) as the major component of the residual sediment, with very small amounts of clastic material. Sediment C/N atomic ratio values do not exceed 14, suggesting that most of the sediment deposited in the lake is of aquatic origin. Variations in the relative contribution of aragonite, organic, and residual materials are expressed as visible changes in sediment color caused by the sharp contrast between the dominant sediment facies (*SI Materials and Methods*). Digital images of the 6,000-yr laminated core section were obtained under controlled light conditions to quantify these color changes by extracting a grayscale reflectance record, which was generated through averaging of the red-green-blue color bands (ref. 36 and Fig. S7). As is common for grayscale measurements, high water content and frozen-sediment processing techniques reduced contrast between laminations and altered color values for the period after approximately 1850 A.D., which corresponds to the time period covered by the freeze core. Consequently, this portion of the record was excluded from grayscale analysis.

δ^{18}O and δ^{13}C analyses of aragonite were performed on the finely laminated sediment, which was sampled at 2–3 mm resolution (approximately 5 yr/sample), as well as modern carbonates, which were captured with a sediment trap deployed from 2005 to 2006 (*SI Materials and Methods*). Stable isotope results show correlation between δ^{18}O and δ^{13}C ($n = 1210$, $r = 0.72$, $p < 0.0001$) (Fig. S8). This relationship is common in closed-basin lakes (37), where carbonate δ^{18}O is primarily controlled by P/E. However, the degree of this control varies, as the ratio between surface area and volume does not change linearly with lake level (38). The Castor Lake volume, outseepage rate, and surface area to volume ratio profile are such that the isotopic balance of the lake is more sensitive to annual to decadal-scale precipitation variability than to mean state precipitation changes (10,11). For a given reduction in mean precipitation, the isotope values shift rapidly, but in the absence of further change gradually return to a steady state representative of the new mean precipitation value, with large shifts in the isotopic baseline requiring very large changes in mean precipitation. The nature of the sensitivity of this proxy makes it well suited for examining changes in P/E variability at approximately 5 yr resolution, which matches the sampling interval. Water temperature is an additional factor in controlling carbonate isotopic composition, but in Castor Lake temperature effects on the isotopic record can be dismissed as the dominant control because of the large magnitude of change in isotope values. A 2‰ shift would require an average summer temperature change of approximately 6 °C (39), unrealistic under any Holocene scenario (40). In analogous systems, these confounding influences are far outweighed by changes in lake volume governed by changing P/E (41).

ACKNOWLEDGMENTS. We thank Jeremy Moberg, Chris Helander, and Dale Swedberg. This work was supported by National Science Foundation Grant ATM-0401948.

1. Cook ER, Woodhouse CA, Eakin CM, Meko DM, Stahle DW (2004) Long-term aridity changes in the western United States. *Science* 306:1015–1018.
2. Seager R (2007) The turn of the century North American drought: Global context, dynamics, and past analogs. *J Climate* 20:5527–5552.
3. Fuchs B (2009) *US Drought Monitor* (National Centers for Environmental Prediction/National Weather Service/NOAA, Climate Prediction Center) available at http://drought.unl.edu/dm/monitor.html.
4. McCabe GJ, Palecki MA, Betancourt JL (2004) Pacific and Atlantic Ocean influences on multidecadal drought frequency in the United States. *Proc Natl Acad Sci USA* 101:4136–4141.
5. Allen M, Ingram WJ (2002) Constraints on future changes in climate and the hydrologic cycle. *Nature* 419:224–232.
6. Cook ER, Meko DM, Stahle DW, Cleaveland MK (1999) Drought reconstructions for the continental United States. *J Climate* 12:1145–1162.
7. Gedalof Z, Peterson DL, Mantua NJ (2005) Atmospheric, climatic, and ecological controls on extreme wildfire years in the northwestern United States. *Ecol Appl* 15:154–174.
8. Knapp PA, Soulé PT, Grissino-Mayer HD (2004) Occurrence of sustained droughts in the interior Pacific Northwest (A.D. 1733-1980) inferred from tree-ring data. *J Climate* 17:140–150.
9. Cook ER, Meko DM, Stahle DW, Cleaveland MK (2004) North American summer PDSI reconstructions: IGBP PAGES/World Data Center for Paleoclimatology, Data Contribution Series # 2004-045. (NOAA/NGDC Paleoclimatology Program, Boulder, CO).
10. Steinman BA, Rosenmeier MF, Abbott MB, Bain DJ (2010) The isotopic and hydrologic response of small, closed-basin lakes to climate forcing from predictive models: Application to paleoclimate studies in the upper Columbia River basin. *Limnol Oceanogr* 55:2231–2245.
11. Steinman AB, Rosenmeier MF, Abbott MB (2010) The isotopic and hydrologic response of small, closed-basin lakes to climate forcing from predictive models: Simulations of stochastic and mean-state precipitation variations. *Limnol Oceanogr* 55:2246–2261.
12. Gibson JJ, Prepas EE, McEachern P (2002) Quantitative comparison of lake throughflow, residency, and catchment runoff using stable isotopes: modeling and results from a regional survey of Boreal lakes. *J Hydrol* 262:128–144.
13. Palmer WC (1965) Meteorological drought, Research Paper No. 45: US Weather Bureau. (Office of Climatology, US Weather Bureau, Washington DC).
14. Shapley MD, Ito E, Donovan JJ (2005) Authigenic calcium carbonate flux in groundwater-controlled lakes: Implications for lacustrine paleoclimate records. *Geochim Cosmochim Ac* 69:2517–2533.
15. Mantua NJ, Hare SR (2002) The Pacific Decadal Oscillation. *J Oceanogr* 58:35–44.
16. Torance C, Compo GP (1998) A practical guide to wavelet analysis. *B Am Meteorol Soc* 79:61–78.
17. Gedalof Z, Smith DJ (2001) Dendroclimatic response of mountain hemlock (*Tsuga mertensiana*) in Pacific North America. *Can J Forest Res* 31:322–332.
18. Benson L, et al. (2003) Influence of the Pacific Decadal Oscillation on the climate of the Sierra Nevada, California, and Nevada. *Quaternary Res* 59:151–159.
19. MacDonald GM, Case RA (2005) Variations in the Pacific Decadal Oscillation over the past millennium. *Geophys Res Lett* 32:L08703.
20. Bryson RA, Hare KF, eds. (1974) *Climates of North America* (Elsevier, New York), 11 p 420.
21. Cayan DR, Dettinger MD, Diaz HF, Graham NE (1998) Decadal variability of precipitation over western North America. *J Climate* 11:3148–3166.
22. Mantua NJ, Hare SR, Zhang Y, Wallace JM, Francis RC (1997) A Pacific interdecadal climate oscillation with impacts on salmon production. *B Am Meteorol Soc* 78:1069–1079.
23. Biondi F, Gershunov A, Cayan DR (2001) North Pacific decadal climate variability since 1661. *J Climate* 14:5–10.
24. D'Arrigo R, Wilson R (2006) On the Asian expression of the PDO. *Int J Climatol* 26:1607–1617.
25. Shen C, Wang WC, Gong W, Hao Z (2006) A Pacific Decadal Oscillation record since 1470 A.D. reconstructed from proxy data of summer rainfall over eastern China. *Geophys Res Lett* 33:L03702.

GEOLOGY

26. Trenberth KE, Hurrell JW (1994) Decadal atmosphere-ocean variations in the Pacific. *Clim Dynam* 9:303–319.
27. Seager R, Kushnir Y, Herweijer C, Naik N, Velez J (2005) Modeling of tropical forcing of persistent droughts and pluvials over western North America: 1856-2000. *J Climate* 18:4065–4088.
28. Verdon DC, Franks SW (2006) Long-term behavior of ENSO: Interactions with the PDO over the past 400 years inferred from paleoclimate records. *Geophys Res Lett* 33:L06712.
29. Newman M, Compo GP, Alexander MA (2003) ENSO-forced variability of the Pacific Decadal Oscillation. *J Climate* 16:3853–3857.
30. Koutavas A, deMenocal PB, Olive GC, Lynch-Stieglitz J (2006) *Geology* 34:993–996.
31. Tudhope AW, et al. (2001) Variability in the El Niño-Southern Oscillation through a glacial-interglacial cycle. *Science* 291:1511–1517.
32. Moy CM, Seltzer GO, Rodbell DT, Anderson DM (2002) Variability of El Niño/Southern Oscillation activity at millennial timescales during the Holocene epoch. *Nature* 420:162–165.
33. Donders TH, Wagner-Cremer F, Visscher H (2008) Integration of proxy data and model scenarios for the mid-Holocene onset of modern ENSO variability. *Quaternary Sci Rev* 27:571–579.
34. Collins M, et al. (2010) The impact of global warming on the tropical Pacific Ocean and El Niño. *Nat Geosci* 3:391–397.
35. Stuiver M, Reimer PJ, Braziunas TF (1998) High-precision radiocarbon age calibration for terrestrial and marine samples. *Radiocarbon* 40:1127–1151.
36. Peterson LC, Haug GH, Hughen KA, Rohl U (2000) Rapid changes in the hydrologic cycle of the Tropical Atlantic during the last glacial. *Science* 290:1947–1951.
37. Talbot MR (1990) A review of the paleohydrological interpretation of carbon and oxygen isotopic ratios in primary lacustrine carbonates. *Chem Geol* 80(Isotope Geology Section):261–279.
38. Benson L, White LD, Rye R (1996) Carbonate deposition, Pyramid Lake subbasin, Nevada: 4. Comparison of the stable isotope values of carbonate deposits (tufas) and the Lahontan lake-level record. *Palaeogeogr Palaeoclimatol Palaeoecol* 122:45–76.
39. Kelts K, Talbot MR (1990) Lacustrine carbonates as geochemical archives of environmental change and biotic/abiotic interactions. *Large Lakes: Ecological Structure and Function*, eds MM Tilzer and C Serruya (Springer, New York), pp 288–315.
40. Rosenberg SM, Walker IR, Mathewes RW, Hallett DJ (2004) Midge-inferred Holocene climate history of two subalpine lakes in southern British Columbia, Canada. *The Holocene* 14:258–271.
41. Benson L, Paillet F (2002) HIBAL: A hydrologic-isotopic-balance model for application to paleolake systems. *Quaternary Sci Rev* 21:1521–1539.